

Macro- and Microphase Transitions in Binary Blends of Block Copolymers with Complementarily Asymmetric Compositions[†]

Daisuke Yamaguchi, Mikihiro Takenaka, Hirokazu Hasegawa, and Takeji Hashimoto*

Department of Polymer Chemistry, Graduate School of Engineering, Kyoto University, Kyoto 606-8501, Japan

Received July 25, 2000; Revised Manuscript Received December 29, 2000

ABSTRACT: A unique phase transition between the state of “two macrophase-separated disordered phases” at higher temperatures and that of “a single phase with only a local order” at lower temperatures was observed in a binary mixture of polystyrene (PS)-*block*-polyisoprene (PI) copolymers by using small-angle X-ray scattering, light scattering, transmission electron microscopy, and optical microscopy. The constituent block copolymers of the mixture have almost same molecular weights but complementary compositions: one component (designated as i-2K) has a number-average molecular weight (M_n) of 1.2×10^4 and its volume fraction of PS (f_{PS}) is 0.81, and the other component (designated as s-3K) is $M_n = 1.3 \times 10^4$ and $f_{PS} = 0.21$; both neat i-2K and neat s-3K are in disordered state at all temperatures covered in this experiment. The macrophase transition temperature for the i-2K/s-3K = 50/50(wt %/wt %) mixture was determined to be 130 °C, above which the mixture showed the two macrophase-separated disordered phases composed of i-2K-rich domains with micrometer size in disordered state and the s-3K-rich domains also in the disordered state. However, when the temperature was sufficiently lower than 130 °C, i-2K and s-3K mixed on the molecular level without involving the macrophase separation to form the single phase composed of locally ordered PS- and PI-rich domains with nanometer size. This phenomenon reveals a “pseudo-LCST type phase diagram” based on the polymer components with a UCST type interaction parameter vs temperature relationship. This phenomenon is intriguing also from the viewpoint that the local segregation of the PS and PI segments induced by increasing the repulsive segmental interactions suppress the macroscopic phase separation between the two compositionally complementary block copolymers in disordered state.

I. Introduction

Diblock copolymers have received considerable experimental and theoretical attention due to their interesting and potentially useful properties, associated with the order–disorder transition (ODT) and the wide array of morphologies in the ordered state.^{1,2} Recently binary blends of A–B diblock copolymers, denoted as (A–B)_α/(A–B)_β, have also received much experimental^{3–19} and theoretical attention,^{20–26} because they show a broad array of interesting behavior, including macrophase separation,^{5,17} microphase separation,^{3,4,8–16,18,19} macrophase separation induced by microphase separation,^{6,7} order–order transitions,^{10–12,16} and modulated or superlattice structures.⁷

As for the (A–B)_α/(A–B)_β in which both copolymers have almost the same total molecular weights, but different compositions (i.e., different A-block fractions), many experimental studies have been conducted for the purpose of controlling the morphology by changing the blend composition. In the earlier works, Hadzioannou and Skoulios investigated the morphological transition from lamellar to cylinder using several sets of binary mixtures of polystyrene-*block*-polyisoprene (PS–PI) copolymers, each of which is a di- or triblock copolymer and possesses lamellar or PS-cylindrical morphology.³ Koizumi et al.⁷ and Vilesov et al.⁸ independently reported that the mixture of equal amounts of two cylinder-forming A–B diblock copolymers, where one is

an A-rich copolymer and forms B-cylinders in A-matrix and the other is a B-rich copolymer and forms A-cylinders in B-matrix, clearly shows a regular lamellar morphology. In these studies, Vilesov et al. used polystyrene-*block*-polybutadiene (PS–PB) copolymers and Koizumi et al. used PS–PI copolymers.^{7,8} Zhao et al.¹¹ investigated the phase behavior of binary blends of PE-PEE (poly(ethylene)-*block*-poly(ethylene)) diblock copolymers with different compositions with an aim of controlling the overall composition very precisely. Sakurai et al. examined the bicontinuous gyroid structure for the binary blends of PS–PI diblock copolymers in detail.¹⁶

Another interest in this type of blends, i.e., the binary blends of A–B polymers having same molecular weights but different compositions, is the complicated superlattice structures as a consequence of the interplay of macrophase separation between the two constituent copolymers of the blend and subsequent microphase separation between A- and B-block chains. Koizumi et al. examined this superlattice structure for a binary blend of PS–PI diblock copolymers.^{7,27}

On the theoretical side, Shi and Noolandi²⁴ or Matsen and Bates²⁶ calculated phase diagram for the (A–B)_α/(A–B)_β, having the same total number of segments, N , but different A-block fractions, i.e., $f_{A,α} \neq f_{A,β}$, by using self-consistent field (SCF) theory. Matsen and Bates²⁶ presented an interesting behavior when the A-block fractions of constituent diblock copolymers are rather different. That is, when $f_{A,α} = 1 - f_{A,β} = 0.2$, the two copolymers, α and β, at first undergo macrophase separation into two disordered phases, and then mix to form a single microphase-separated structure, with increasing χN from the disordered single phase.²⁶ Here

* To whom correspondence should be addressed.

[†] Presented in part at the 48th Symposium of the Society of Polymer Science, Japan, Oct. 1999. *Polym. Prepr. Jpn., Soc. Polym. Sci., Jpn.* 1999, 48, 2179–2180.

Table 1. Characteristics of PS-PI Diblock Copolymers

code	M_n	$M_{n,PS} - M_{n,PI}^a$	M_w/M_n	f_{PS}^b
i-2K	1.2×10^4	$1.0 \times 10^4 - 2 \times 10^3$	1.06	0.81
i-3K	1.3×10^4	$1.0 \times 10^4 - 3 \times 10^3$	1.05	0.75
s-3K	1.3×10^4	$3 \times 10^3 - 1.0 \times 10^4$	1.07	0.21

^a $M_{n,k}$ is the number-average molecular weight of the k th block (k = PS or PI). ^b f_{PS} is the volume fraction of PS block chain, estimated by $f_{PS} = (w_{PS}/\rho_{PS})/[w_{PS}/\rho_{PS} + (1 - w_{PS})/\rho_{PI}]$, where $w_{PS} = M_{n,PS}/M_n$, $\rho_{PS} = 1.0514 \text{ g}\cdot\text{cm}^{-3}$, and $\rho_{PI} = 0.925 \text{ g}\cdot\text{cm}^{-3}$.

χ is the usual Flory-Huggins segmental interaction parameter between A and B segments. This phenomenon seems paradoxical and therefore intriguing, since starting from the macrophase-separated state of α and β copolymers as an initial state, increasing of χN yields mixing of α and β . It *could* never happen, if α and β were B- and A-homopolymer, respectively. However, in the case where both α and β are A-B diblock copolymers and $f_{A,\alpha} = 1 - f_{A,\beta} = 0.2$, it can happen due to the existence of the microphase-separated state. Namely the microphase separation (or local segregation of A and B) suppresses the effective repulsive interactions of α and β in the disordered state which drives the macrophase separation.

Our objective in this paper is to report our experimental observation of a phase transition from a macrophase-separated state of constituent copolymers at high temperatures (i.e., small χN) to a single microphase-separated structure at low temperatures (i.e., large χN) for a binary blend of PS-PI diblock copolymers which have almost same molecular weights and complementarily asymmetric compositions. Although such a phase behavior appears strange, we have checked the reproducibility and confirmed that it is not artificial but natural. Furthermore, this experimental result seems to be in good agreement with the theoretical work by Matsen and Bates.²⁶

II. Experimental Section

II. 1. Sample Preparation. Diblock copolymers, polystyrene (PS)-*block*-polyisoprene (PI), were synthesized by living anionic polymerization with *sec*-butyllithium as an initiator and cyclohexane as a solvent. The polymer molecular weight was characterized by GPC. In each synthesis a precursory sample was taken out before the second step polymerization of PI (or PS) to determine the molecular weight of the PS (or PI) block by GPC. Three SI diblock copolymers were used in this study, two of these are PS-rich copolymers, designated as i-2K and i-3K, and the other one is a PI-rich diblock copolymer, designated as s-3K, where the first letter (i or s) designates the component of the short block (polyisoprene or polystyrene block, respectively) and the second number the molecular weight of the short block in units of thousand. In all cases the polydispersity index, M_w/M_n , was relatively small ($M_w/M_n \leq 1.07$). The characteristics of these PS-PI copolymers are summarized in Table 1.

Film specimens were cast from a 5 wt % polymer in toluene solution. 0.5 wt % of antioxidant (Irganox 1010, Ciba-Geigy Group) was added to the solution to prevent the thermal degradation of the film specimens during the following measurements. Two blend samples of the block copolymers of i-2K and s-3K or i-3K and s-3K were prepared and designated as i-2K/s-3K = 50/50 and i-3K/s-3K = 50/50, respectively, where 50/50 denotes the weight ratio of the two block copolymers in the blends.

II. 2. Small-Angle X-ray Scattering. Each neat diblock copolymer and blend sample was measured *in-situ* as a function of temperature with small-angle X-ray scattering (SAXS) with the apparatus described elsewhere, except for the replacement of the X-ray generator with a new one (MAC

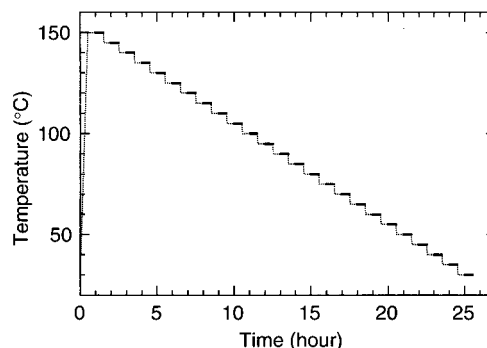


Figure 1. Typical thermal protocol given in the SAXS experiments. For neat diblock copolymers and blend samples, all the measurements were conducted during cooling process as presented here. The thick solid line designates the period of measurement.

Sciences M18X HF operated at 18 kW).²⁸⁻³⁰ All measurements were conducted with specimens placed in a nitrogen atmosphere to reduce oxidative degradation. The typical thermal protocol employed in the SAXS experiments is schematically shown in Figure 1. Although the SAXS experiments of only the cooling process will be shown and discussed in this paper, heating or isothermal annealing processes will be also discussed with respect to light-scattering and optical microscopy experiments, as will be detailed later. At each temperature, the specimen was held for 30 min before the measurement and the measurement lasted for 30 min. SAXS profiles were desmeared for slit-width and slit-height smearing and corrected for air scattering, absorption, and thermal diffuse scattering.²⁸⁻³⁰ The absolute intensity was obtained by the nickel-foil method.³¹

II. 3. Transmission Electron Microscopy. Microphase- or macrophase-separated morphologies of the blend specimens were observed by transmission electron microscopy (TEM). For the TEM observation, the film specimens were microtomed at -100°C , using a Reichert Ultracut E low-temperature sectioning system. The ultrathin sections were stained with the vapor of 2% $\text{OsO}_4(\text{aq})$ for a few hours.³² The observation was done with a JEOL JEM-2000FXZ transmission electron microscope operated at 120 kV. The thermal protocols of the specimens used for TEM observations are described in the following section, section III. 2.

II. 4. Light Scattering. Temperature-dependent macrophase-separated structure was investigated *in-situ* by using time-resolved elastic light-scattering (LS). He-Ne laser of 20 mW power ($\lambda_0 = 632.8 \text{ nm}$, where λ_0 is the wavelength of light in the vacuum) was used as an incident beam source, and the light scattering was observed photometrically. Further details of the apparatus were described elsewhere.³³ The thermal protocols employed in the LS experiments are described in the following section, section III. 3.

II. 5. Optical Microscopy. The macrophase-separated structures were also observed under optical microscopy (OM). The specimen was placed in a conventional optical microscope and the observation was carried out under a magnification of $\times 100$.

III. Results and Discussion

III. 1. SAXS. In Figure 2, we show the SAXS profiles for the three neat diblock copolymers (a) i-2K, (b) i-3K, and (c) s-3K at various temperatures, where q is the magnitude of scattering vector defined by $q = (4\pi/\lambda) \sin(\theta/2)$ with λ and θ being the wavelength of X-ray and the scattering angle, respectively. For each neat block copolymer, the scattered intensity increases with decreasing temperature, indicating that the composition fluctuation increases as a consequence of increasing segregation power between PS-block and PI-block with decreasing temperature. However, in each profile, there

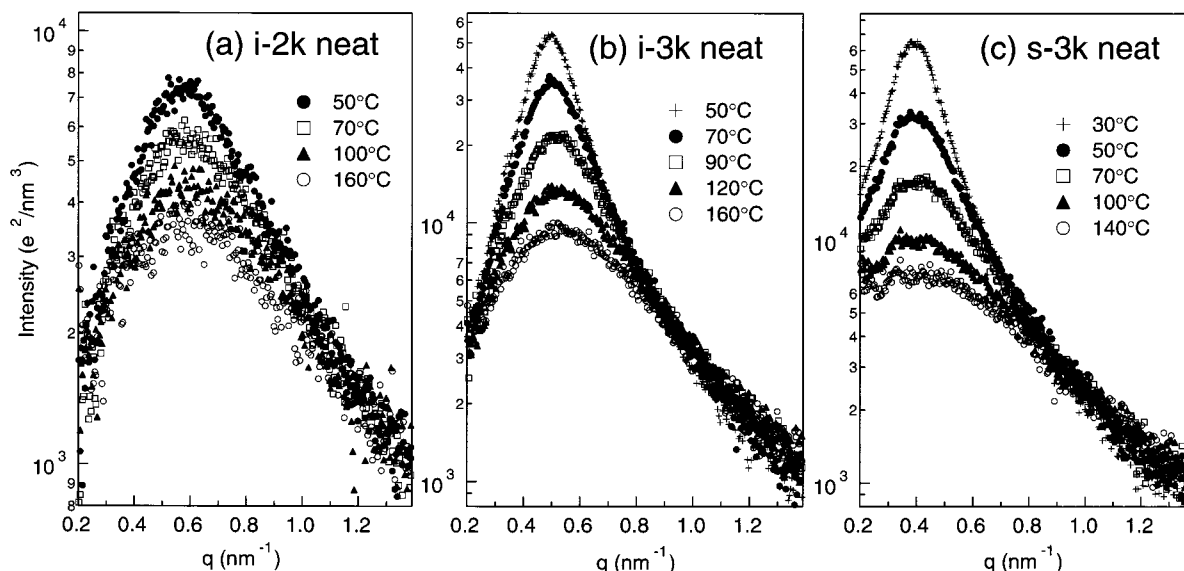


Figure 2. Temperature dependence of the SAXS profiles for neat diblock copolymers: (a) i-2K; (b) i-3K; (c) s-3K.

exists only one broad scattering peak even at the lowest temperature, indicating that all of the three neat copolymers employed in this study remain in the disordered state at the temperature range investigated here.

In Figure 3, we give plots of (a) the reciprocal of the peak intensities (I_m^{-1}) vs the reciprocal of the absolute temperature (T^{-1}), and (b) the square of the half-width at half-maximum (σ_q^2) of the scattering peak for each neat block copolymer. All the curves for I_m^{-1} and σ_q^2 in Figure 3, parts a and b, continuously decrease with increasing T^{-1} , supporting the consideration that three neat copolymers, i-2K, i-3K, and s-3K, are in the disordered state at all temperature range investigated in this study. Note that the curves of i-2K and i-3K, denoted by the symbols \bullet and \blacktriangle , respectively, show a slope change at $T^{-1} \approx 3.1 \times 10^{-3}$ (i.e., $T \approx 50^\circ\text{C}$), probably due to the glass transition temperature (T_g) of the specimens.^{34,35}

In Figure 4, we show the SAXS profiles of i-2K/s-3K = 50/50 at various temperatures. The behavior of SAXS profiles with decreasing temperature observed in Figure 4 is quite different from those observed in Figure 2, parts a and c, for the corresponding constituent neat copolymers. At temperatures above 130°C , the SAXS profiles for the blend do not have any distinct scattering maxima but show a monotonic decrease of scattering intensity with increasing q , as shown in Figure 4a. However, as the temperature is decreased to 120°C , a broad scattering maximum appears in the SAXS profile at $q \approx 0.1\text{ nm}^{-1}$ and it becomes sharper and shifts toward larger q with further decreasing temperature, as shown in Figure 4b. This temperature behavior of the SAXS profiles for the blend strongly suggests the macrophase separation between i-2K and s-3K at temperatures above 130°C , which will be discussed in more detail in the following sections, sections III. 2. and III. 3.

Note that one might think that even if the macrophase separation between i-2K and s-3K occurs at the temperatures above 130°C , the SAXS profiles at these temperatures should possess the scattering maxima corresponding to the neat copolymers of i-2K and s-3K, as shown in Figure 2, parts a and c, respectively. However, when the macrophase-separated structures

exist in the system, the excess scattering arising from the macrophase-separated domains region appears in the small q region of SAXS profile. This excess scattering is strong and may cover the broad and weak scattering maxima originating from the composition fluctuations of constituent copolymers, i-2K and s-3K, within each domains.

In Figure 5, we show the SAXS profiles of i-3K/s-3K = 50/50 at various temperatures. In this case, the scattering maximum arising from the composition fluctuations with nanometer sizes is observed, and there is no evidence of macrophase separation at any temperatures up to 150°C as evidenced by no excess scattering in the small q region, indicating that the constituent copolymers, i-3K and s-3K, are mixed on the molecular level. However, anomalous behavior is observed in regard to the peak shift with temperature change. The scattering maximum from this blend locates at $q = 0.21\text{ nm}^{-1}$ at 150°C and shifts toward larger q with decreasing temperature. This behavior is similar to that observed in i-2K/s-3K = 50/50 and quite different from that observed in constituent neat copolymers, i-3K and s-3K.

To compare all the behaviors concerning the peak shift with temperature observed in this study, in Figure 6 we give the plots of wavelength of the dominant mode of the spatial composition fluctuations in disordered state (or domain spacing in the case of ordered state), D , defined by $D = 2\pi/q_m$ as a function of T^{-1} . Here q_m is the magnitude of the scattering vector at the scattering maximum. The three neat copolymers show similar behavior in D vs T^{-1} : The D values for the neat copolymers definitely increase with decreasing temperature, though the change of D with temperature is much small compared with that for the blends. This tendency for the neat diblock copolymers is consistent with that reported earlier³⁶ and attributed to the increasing chain stretching caused by the increase of repulsive interactions between PS and PI blocks with decreasing temperature.

In contrast to the three neat copolymers, the two blend specimens, i.e., i-2K/s-3K = 50/50 and i-3K/s-3K = 50/50, exhibit a large decrease of D with decreasing temperature to a point ($\sim T_g$) and then levels off. Although the two blend samples show the same trend

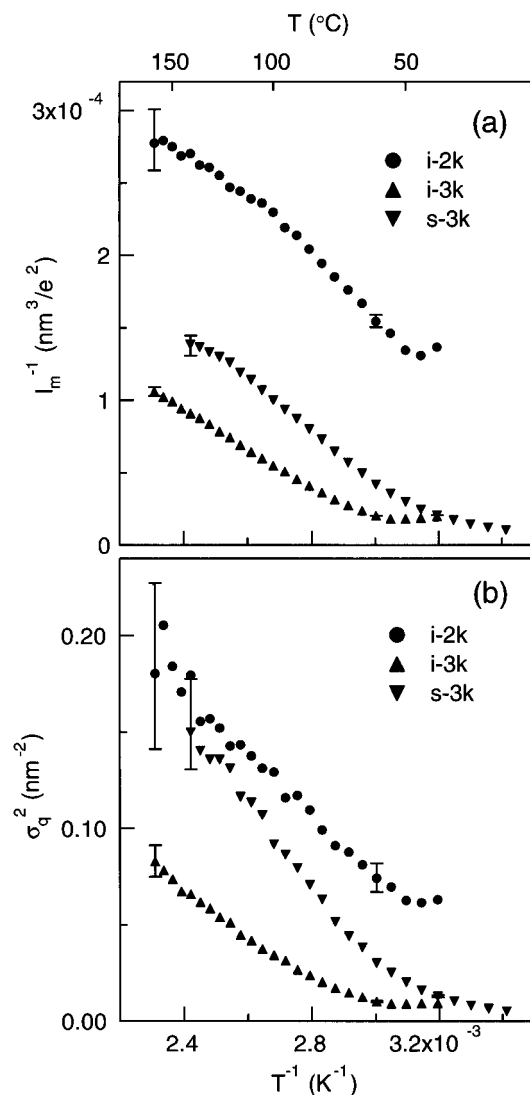


Figure 3. (a) I_m^{-1} (inverse of peak scattered intensity) and (b) σ_q^2 (square of the half-width at half-maximum of the peak) plotted as a function of T^{-1} (inverse of the absolute temperature) for neat diblock copolymers: (●) i-2K; (▲) i-3K; (▼) s-3K.

they are definitely different in the point that whether the macrophase separation between the constituent copolymers play a role on D . Once the macrophase separation of constituent copolymers occurs, the dominant mode of the spatial composition fluctuations in the blend system should also split into those inherent in block copolymers in both phases. However, we could not actually identify the SAXS maximum from each phase, since each of the scattering maximum is overwhelmed by the excess scattering from macrophase-separated structures at $q \approx 0$, and therefore, the data points of D for i-2K/s-3K = 50/50 at high temperatures (above 120 °C) are not shown in Figure 6. On the contrary, the single SAXS scattering maximum exists even at the high-temperature range for the i-3K/s-3K = 50/50 mixture, reflecting no macrophase separation. It is quite remarkable that the values of D reach 50 and 30 nm at higher temperatures for i-2K/s-3K = 50/50 and i-3K/s-3K = 50/50, respectively, despite the fact that the values of D for each individual neat copolymer, i-2K, i-3K, and s-3K, are ≈ 10 , 12, and 15 nm, respectively.

It is worthy to note here about the experimental results reported earlier by Sakurai et al.¹⁵ They found a similar unusual temperature behavior of D for the

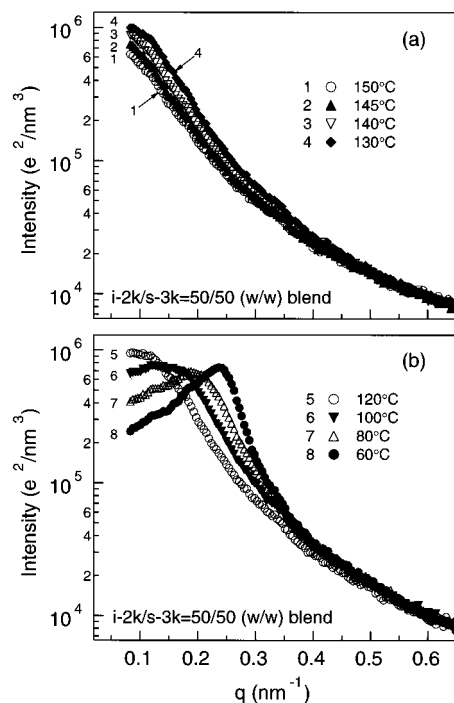


Figure 4. Temperature dependence of the SAXS profiles for the i-2K/s-3K = 50/50 blend. Parts a and b give, respectively, the change in the profiles above 130 °C (where i-2K and s-3K are considered to be phase-separated) and that below 120 °C (where i-2K and s-3K are considered to be mixed on the molecular level).

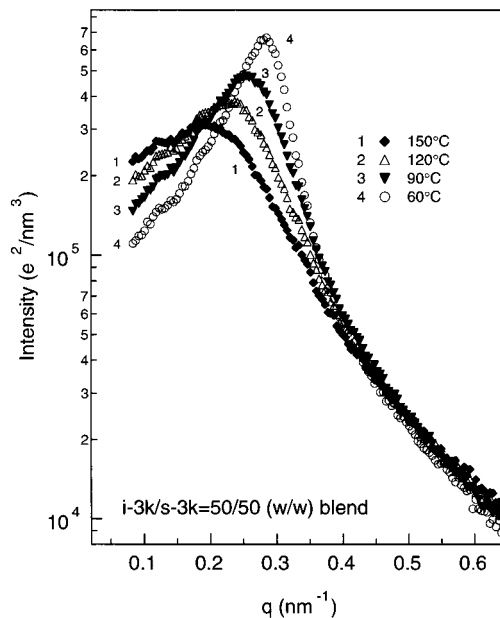


Figure 5. Temperature dependence of the SAXS profiles for the i-3K/s-3K = 50/50 blend. The blend is considered to be miscible at the whole temperature range below 150 °C.

lamellar microdomains with long-range order in the binary mixture of SI diblock copolymers. One might notice that the unusual behavior found earlier by Sakurai et al.¹⁵ is quite identical with the temperature dependence of D observed in this study, for i-2K/s-3K = 50/50 and i-3K/s-3K = 50/50, except for the morphological difference between the two cases. However, this morphological difference is responsible for the difference in interpretation of the unusual behavior of D . Namely, Sakurai et al. speculated on the origin of the unusual

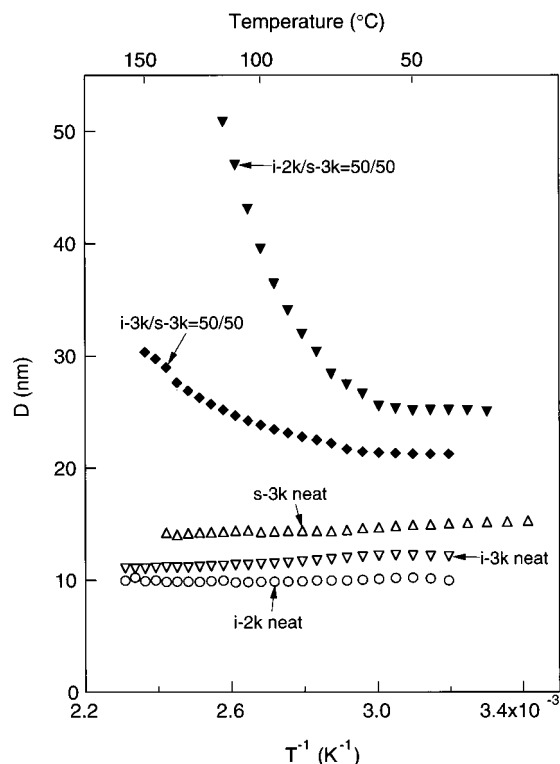


Figure 6. Plot of D , which represents the characteristic length of the dominant mode of the spatial composition fluctuations in the disordered state (or domain spacing in the case of ordered state), as a function of T^{-1} for both neat diblock copolymers and blend samples: (○) i-2K neat; (▽) i-3K neat; (△) s-3K neat; (▼) i-2K/s-3K = 50/50 blend; (◆) i-3K/s-3K = 50/50 blend.

behavior of D as follows: as the temperature increases, the enhancement of the miscibility between the PS and PI block chains causes the undulation of interface between PS and PI lamellar microdomains. As the interface undulates, the longer PS and PI block chains in each constituent copolymer are stretched in the direction normal to lamellar interface to prevent chain overlaps, leading to larger domain spacing.¹⁵ This speculation seems interesting, but we cannot apply it to our results, since in our case the specimens are in disordered state and the interface between PS and PI microdomains is nonsense. At present we do not have a clear image which can interpret the behavior of D observed in i-2K/s-3K = 50/50 or i-3K/s-3K = 50/50 reasonably.

III. 2. TEM. TEM observations were conducted to explore the self-assembled structures formed in i-2K/s-3K = 50/50 or i-3K/s-3K = 50/50. To compare the state at high temperatures with that at low temperature, we used two different types of thermal protocols for both i-2K/s-3K = 50/50 and i-3K/s-3K = 50/50. One thermal protocol is hereafter designated as "rapidly quenched" from 150 °C and gives the following process: as-cast specimen is elevated from ambient temperature to 150 °C and annealed at 150 °C for 1.5 h followed by a rapid quenching in ice water.³⁷ This thermal protocol will qualitatively reflect the state of the blends typically at high temperatures. The other thermal protocol is hereafter designated as "slowly cooled", also from 150 °C and gives the following process: as-cast specimen is elevated from ambient temperature to 150 °C and annealed at 150 °C for 1 h followed by stepwise cooling to ambient temperature just as schematically depicted in Figure

1. This protocol will reflect the state of the blends typically at low temperatures. We prepared ultrathin sections from the specimen used for SAXS measurements. In cooling process from 150 °C, each temperature decrement is 5 °C/h.

In Figure 7, we show the TEM micrographs obtained from the observation of i-2K/s-3K = 50/50. Parts a–d of Figure 7 show the micrographs of the rapidly quenched specimen, while parts e–h of Figure 7 show those of the slowly cooled specimen. As shown in Figure 7a taken at low magnification, we can find the macrophase-separated structures in the rapidly quenched specimen. This observation seems in good agreement with the SAXS results shown in Figure 4a. A lot of bright ellipsoidal domains with their sizes from several micrometers to 10 μm are dispersed in the dark matrix. Since the ultrathin sections were stained with OsO₄, the bright and dark parts correspond to PS- and PI-rich phases, respectively, implying that the bright phase and the dark phase are rich in i-2K and s-3K, respectively. Both the dark and bright phases have intricate contrast variation, reflecting a seemingly bicontinuous structure. The enlarged images obtained by zooming in on inside of the each phase and interface area are shown in Figure 7, parts b–d, respectively. Inside of the s-3K-rich phase, a faint contrast exists in the dark background (Figure 7b). This faint contrast implies that there exist the spatial composition fluctuations in the matrix phase with the size of tens of nanometers, suggesting that this phase is in the disordered state. Similarly a faint contrast exists in the bright background, implying existence of the spatial composition fluctuations inherent in the disordered state within the i-2K-rich phase (Figure 7c). Further, it seems that the amplitude of the composition fluctuation in the i-2K-rich phase (Figure 7c) is smaller than that in the s-3K-rich phase (Figure 7b), consistent with the fact that the SAXS peak intensity of i-2K is smaller than that of s-3K as shown in Figure 2, parts a and c. Note that there exist dark stripes in Figure 7c as well as in Figure 7, parts d, g, and h. They are chatter marks of the ultrathin sections which are artifacts brought during microtoming.³⁸ The interface between the two phases (upper-right region of Figure 7d) seems relatively sharp.

We can observe the macroscopically phase-separated structure in the specimen slowly cooled from 150 °C, as shown in Figure 7e, contrary to our expectations based on the SAXS results shown in Figure 4b. However, comparing Figure 7e with 7a, one can notice the big differences between them: the domains observed in the slowly cooled specimen are much larger in average size and much smaller in number density compared with that observed in the rapidly quenched specimen. Further, we can find additional differences between the rapidly quenched specimen and slowly cooled specimen in Figure 7, parts f–h, which are obtained by zooming in on parts of Figure 7e, namely, inside of the dark phase, inside the bright phase, and the interface area between these phases, respectively.

Inside of the dark phase of the slowly cooled specimen, we can observe a fairly sharp contrast, suggesting a large amplitude of the thermal composition fluctuations (Figure 7f). Contrary to Figure 7b, Figure 7f shows the bright area as much as the dark area. This suggests that the matrix phase of slowly cooled specimen contain considerable amount of the PS-rich copolymer (i-2K) as well as the PI-rich copolymer (s-3K). Besides the large

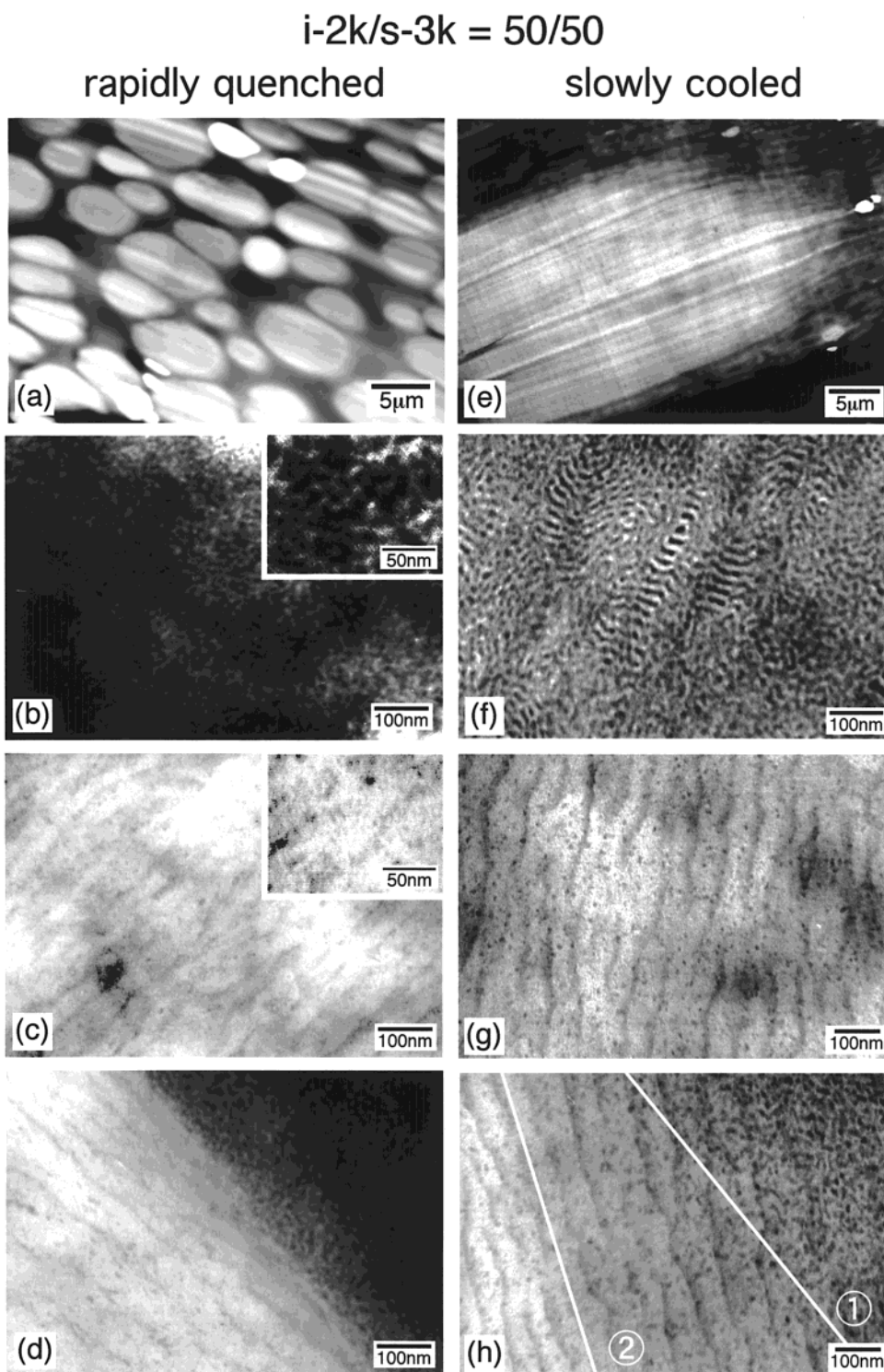


Figure 7. TEM micrographs of the $i\text{-}2K/s\text{-}3K = 50/50$ blend. Parts a–d and parts e–h, respectively, correspond to the specimen rapidly quenched from 150 to 0 °C and that slowly cooled from 150 °C to room temperature. The top two micrographs (a and e) were taken at low magnification, and the other micrographs were obtained by zooming in on the inside of the dark phase (b and f), the inside of the bright phase (c and g), and the interfacial area between the two phases (d and h). Note that the striations with spacing ≈ 50 nm appearing in parts c, d, g, and h are artifacts introduced by the ultrathin sectioning process.

amplitude of the thermal composition fluctuations, there exist some kind of ordered microdomain structures similar to the alternating lamellar in Figure 7f, also strongly suggesting the existence of both $i\text{-}2K$ and $s\text{-}3K$ copolymers, since $s\text{-}3K$ copolymer will never form that kind of microdomain structure by itself.

On the other hand, internal structures of the bright phase of slowly cooled specimen shown in Figure 7g are

similar to those of quenched specimen as shown in Figure 7c. The difference between parts c and g is that the number of dark PI-rich domains in part g is much larger than that observed in part c. This difference may indicate a larger degree of intermixing of the two components during slow cooling process. Another crucial difference appears in the interfacial area between the two phases. Since the interface in Figure 7h is too broad,

one might not be able to distinguish the interfacial area. However, the upper right side of Figure 7h, where the large number of dark points overlap each other and seem to be somewhat similar to the large amplitude thermal concentration fluctuations as shown in Figure 7f, corresponds to the edge of the dark phase (see the line numbered 1 drawn on the figure) and the lower left side of Figure 7h, which appears bright and similar to the image observed in Figure 7g, corresponds to the edge of the bright phase (see the line numbered 2). Therefore, the central part of Figure 7h, where the density of dark points gradually increases from left side (line 2) to right side (line 1), corresponds to the interfacial area between the two phases. The interface between the two phases observed in the quenched specimen is much sharper than that of the slowly cooled specimen. Hence, we cannot help speculating that the broadening of the interface occurred during the slow cooling process. This strongly suggests that at high temperatures, i.e., about 150 °C, the two constituent copolymers, i-2K and s-3K, tend to phase-separate each other with a sharp interface. As temperature is lowered, i-2K and s-3K tend to become miscible with each other on the molecular level. Consequently, we can speculate further that the macrophase-separated structures observed in the slowly cooled specimen, as shown in Figure 7e, are a consequence of growth of the macrophase-separated domains at high temperatures during the slow cooling process, a subsequent intermixing of the two phases at lower temperature and an eventual freezing due to the cooling below T_g of PS-rich phase and will be destined to disappear with long annealing at temperature slightly above T_g of PS-rich phase. This speculation will be very well substantiated by the LS and OM experiments as will be discussed later in Figures 10, 12, and 13. On the whole, the TEM observation for i-2K/s-3K = 50/50, shown in Figure 7, seems to be consistent with the SAXS result, shown in Figure 4, and both SAXS and TEM results suggest that i-2K and s-3K phase-separate each other at high temperature, while they become miscible with each other at low temperature.

In Figure 8 parts a and b, we show the TEM images of i-3K/s-3K = 50/50 obtained from the specimens rapidly quenched from 150 °C and slowly cooled from 150 °C, respectively. One may notice that there are no macrophase-separated structures in both parts a and b of Figure 8. In fact, for i-3K/s-3K = 50/50, we could not find the macrophase-separated structures such as those observed in i-2K/s-3K = 50/50. If i-3K and s-3K *had been* immiscible at 150 °C and *formed* some kind of macroscopically phase-separated structures, we *could have observed* the traces of them as in the case of i-2K/s-3K = 50/50. The difference of the two blend systems in their phase behavior will be discussed in detail later in section IV. 2.

III. 3. LS and OM. To investigate more about macrophase separation between constituent copolymers, we used LS and OM, which are the most suitable methods for the observation of the structures with micron size. We have conducted two kinds of experiments with LS; one, hereafter designated as "heating experiment", is to determine the macrophase transition temperature of the blend samples, and the other, hereafter designated as "annealing experiment", is to confirm the miscibility and immiscibility of i-2K and s-3K at lower (70 °C) and higher (150 °C) temperatures. The thermal protocol of each experiment is schemati-

i-3k/s-3k = 50/50

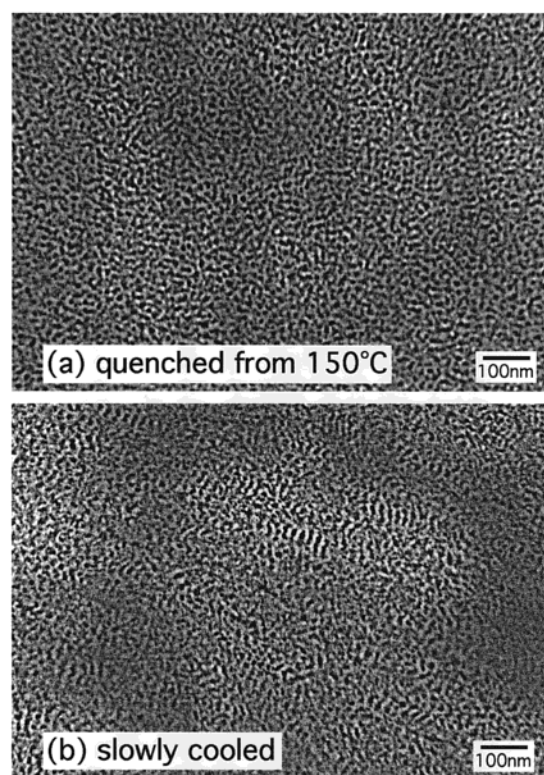


Figure 8. TEM micrographs of the i-3K/s-3K = 50/50 blend. Parts a and b, respectively, correspond to the specimen rapidly quenched from 150 to 0 °C and that slowly cooled from 150 °C to room temperature.

cally shown in Figure 9, parts a and b. As for the heating experiment, an as-cast specimen was first pre-annealed at 70 °C in a vacuum oven for 2 h to remove air bubbles, and then LS measurements were conducted on the heating process at various temperatures from 70 to 130 °C for i-2K/s-3K = 50/50 and from 100 to 150 °C for i-3K/s-3K = 50/50 as shown in Figure 9a. To examine whether the macrophase separation occurs, six scans of the scattered intensity as a function of q , each of which took about 1 min, at intervals of 10 min, were taken at each temperature within the period marked by the thick horizontal line in Figure 9a.

Parts a and b of Figure 10 give the results of the series of photometric scans of the LS scattered intensity for i-2K/s-3K = 50/50 at 125 and 130 °C, respectively. The time shown denotes how many minutes passed after the specimen reached the equilibrium temperature. At 125 °C, all of the LS profiles overlap each other, while at 130 °C the LS profiles show remarkable time dependence; i.e., the intensity at smaller q region increased with time. From these behaviors, we concluded that the macrophase transition temperature exists between 125 and 130 °C on the heating process. In Figure 10c, we show the LS profiles at various temperatures after annealing the blend at the specified temperature for 60 min. There is a big difference between the profiles at 125 (curve 4) and 130 °C (curve 5): whereas all the profiles at the temperatures ranging from 70 to 125 °C (curves 1–4) are almost identical, the profile at 130 °C has a much higher intensity than those at the other temperatures. This temperature dependence of the LS profile confirms that i-2K and s-3K are miscible at the temperatures below 125 °C but phase separate at the temperatures above 130 °C.

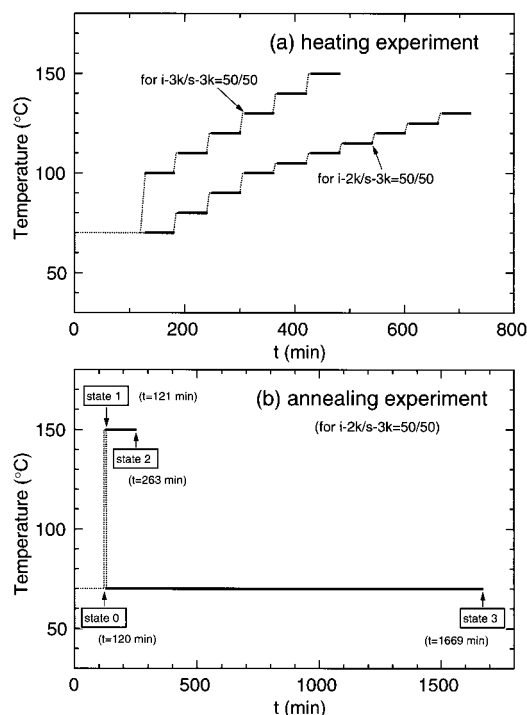


Figure 9. Thermal programs given in the various LS experiments. In part a, the measurements were conducted during a heating process to determine the macrophase transition temperature of the specimen, while in part b, the measurements were conducted during an isothermal annealing at different temperatures to examine the miscibility or immiscibility of the specimen at these temperatures.

Figure 11a shows the time evolution of LS profile for i-3K/s-3K = 50/50 at the highest temperature measured. All the profiles overlap, suggesting that the macrophase separation between i-3K and s-3K does not occur even at 150 °C. In Figure 11b, we show the LS profiles at various temperatures after annealing of the blend for 60 min at the specified temperature. All the profiles are almost identical except for a slight difference due to the fluctuation of the incident beam intensity. Thus, the results of heating experiment for i-3K/s-3K = 50/50, shown in Figure 11b as well as Figure 11a, confirm that i-3K and s-3K do not phase-separate macroscopically, but are miscible with each other at temperatures below 150 °C. We speculate that the specimens remain without the macrophase separation as will be discussed later in section IV. 2. The results will be interpreted later in section IV. 2.

From the heating experiment for i-2K/s-3K = 50/50, we obtain the clear evidence that i-2K and s-3K become immiscible at temperatures higher than 130 °C. However, we have not yet had the clear evidence that after the macrophase separation between i-2K and s-3K at high temperatures, the single phase state of these copolymers is recovered with lowering temperature, although the results from SAXS measurement and/or TEM observation strongly suggest this tendency, as described in the previous sections III. 1 and III. 2. Thus, we examined the thermoreversibility between the single-phase state and the macrophase-separated state of i-2K and s-3K with annealing experiments as described in detail below. In Figure 9b, we give the thermal protocol of the annealing experiment for i-2K/s-3K = 50/50. The blend specimen, which was prepared by freeze-drying from a cyclohexane solution at a polymer concentration of 1% (w/v), was first preannealed for 2 h at 70 °C to

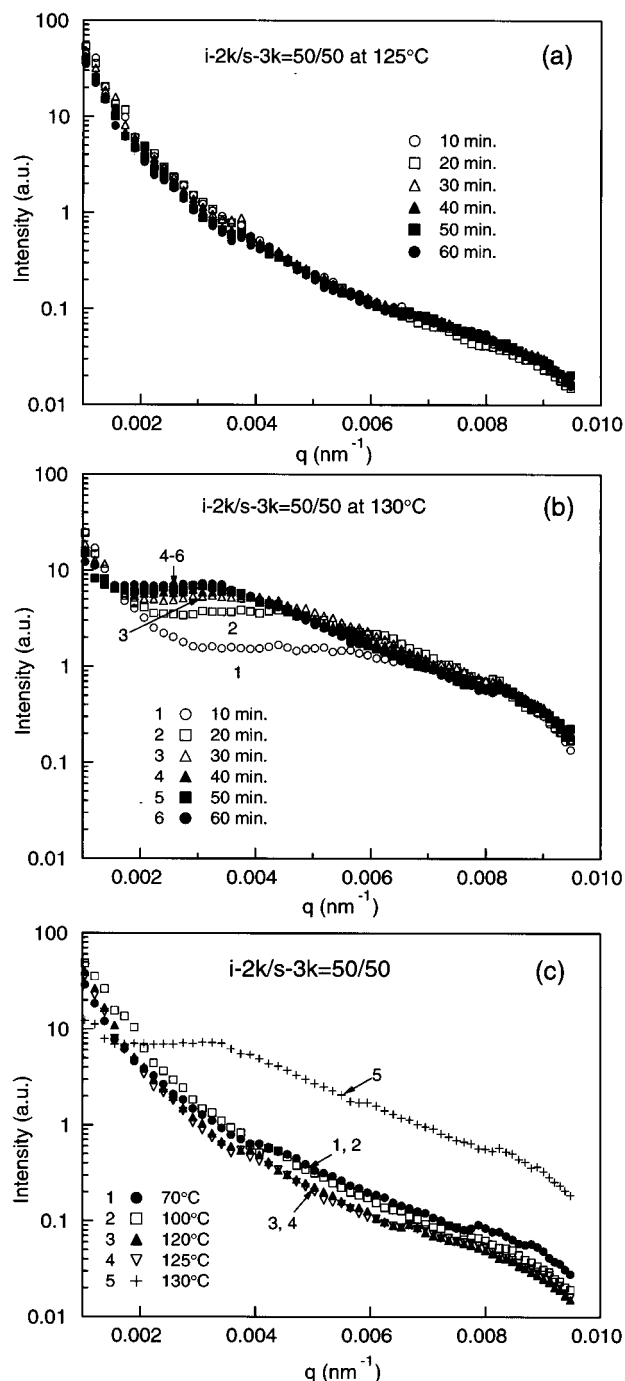


Figure 10. LS profiles for the i-2K/s-3K = 50/50 blend. All the profiles were obtained during the heating process as shown in Figure 9a. Parts a and b give, respectively, time evolution of the profiles at 125 and 130 °C. Part c gives the temperature dependence of the LS profiles measured at 60 min after temperature being incremented to each specified temperature.

remove air bubbles in the sample (which corresponds to "state 0" designated in Figure 9b), and then subjected to an abrupt temperature jump to 150 °C followed by only 1 min annealing at 150 °C to develop phase separation between i-2K and s-3K to a certain degree (which corresponds to "state 1" designated in Figure 9b). The time evolution of LS profiles, from "state 1" as an initial state, were measured during an isothermal annealing process at two different temperatures: one is continuously annealed at 150 °C from $t = 121$ to 263 min (state 2), and the other is an abrupt temperature quench to 70 °C followed by annealing at 70 °C from t

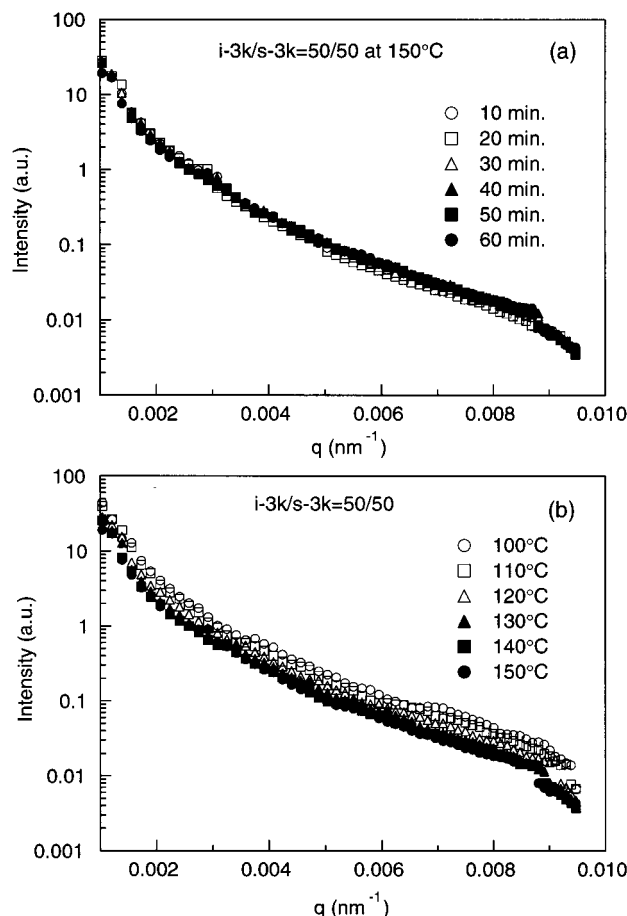


Figure 11. LS profiles for the i-3K/s-3K = 50/50 blend. All the profiles were obtained during the heating process as shown in Figure 9a. Part a gives time evolution of the profiles at 150 °C, while part b gives temperature dependence of the profiles measured at 60 min after temperature being incremented to each specified temperature.

= 121 to 1669 min (state 3), which are marked by thick horizontal lines in Figure 9b.

Comparing the LS profiles at state 0 and state 1 in Figure 12a, we see that only 1 min annealing at 150 °C brought a considerable increase of scattering intensity, due to the macrophase separation between i-2K and s-3K. In Figure 12, parts b and c, we show the time evolution of LS profiles during isothermal annealing at 150 and 70 °C, respectively. Note that the times denoted correspond to those of abscissa of Figure 9b; therefore the actual periods of isothermal annealing at 150 or 70 °C are the times shown in Figure 12, part b or c, minus 121 min. In Figure 12b, we can observe the isothermal phase separation process of i-2K and s-3K at 150 °C. At a first stage (from $t = 121$ to $t = 122$ min), the scattered intensity increases roughly uniformly at the q region ranging from 0.0005 to 0.009 nm^{-1} , indicating the growth of the composition fluctuations for all observed q Fourier modes. Then the scattered intensity further increases with time in the smaller q region, that is $0.0005 \text{ nm}^{-1} \leq q \leq 0.003 \text{ nm}^{-1}$, while the scattered intensity decreases with time (from $t = 126$ to $t = 263$ min) in the larger q region, that is $0.003 \text{ nm}^{-1} \leq q \leq 0.0095 \text{ nm}^{-1}$, suggesting the coarsening of the phase-separated structures with time. On the other hand, we can observe the continuous decrease of the scattered intensity with time (from $t = 122$ to $t = 1669$ min) at the entire q region ranging between $0.001 \text{ nm}^{-1} \leq q \leq$

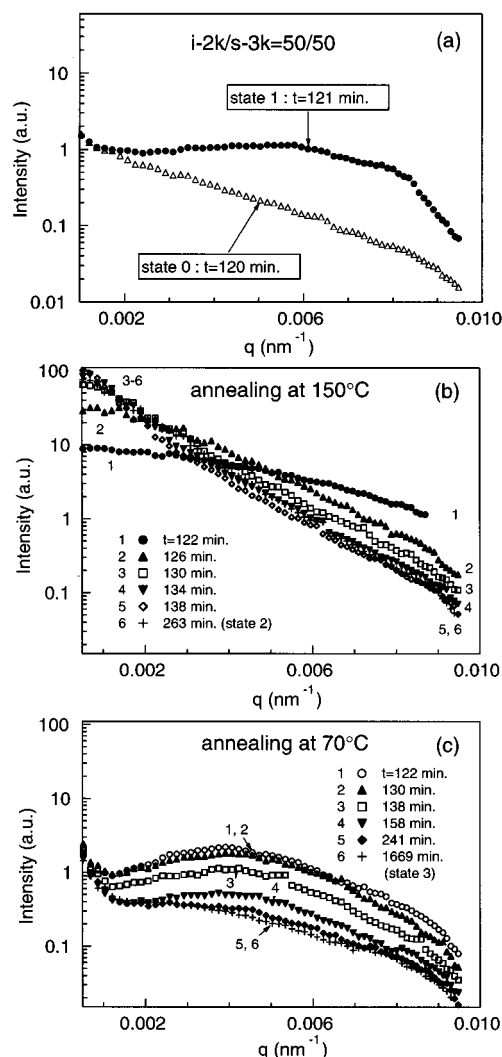


Figure 12. LS profiles of the i-2K/s-3K = 50/50 blend. All the profiles were obtained from the experiments whose thermal programs are given in Figure 9b. Part a gives the profiles before and after 1 min annealing at 150 °C: the annotations, "state 0" and "state 1", correspond to those denoted in Figure 9b. Parts b and c give, respectively, time evolution of the profiles during isothermal annealing at 150 °C and 70 °C: the values of time, shown in parts b and c, are common to those in the abscissa of Figure 9b.

0.0095 nm^{-1} in Figure 12c. This behavior of LS profiles strongly suggests the isothermal mixing of i-2K and s-3K at 70 °C.

Besides the LS measurements, we conducted the real space observation with OM for the i-2K/s-3K = 50/50 specimens used for the annealing experiments with LS. The OM images shown in parts a–c of Figure 13 correspond to states 1–3 of Figure 9b, respectively. The results are consistent with those of LS measurement. The specimen annealed at 150 °C for 1 min (part a) shows a relatively clear fluctuation of refractive index with micrometer sizes, indicating that i-2K and s-3K phase-separated to a certain degree. A continuous annealing at 150 °C for more than 2 h resulted in further coarsening of the phase separation between i-2K and s-3K (Figure 13b), whereas an annealing at 70 °C for more than 1 day on the sample annealed at 150 °C for 1 min erased the initial pattern of the fluctuations of refractive index as shown in Figure 13a, giving rise to a uniform structure with less refractive index fluctuations (Figure 13c). The combined results of LS and

i-2k/s-3k = 50/50

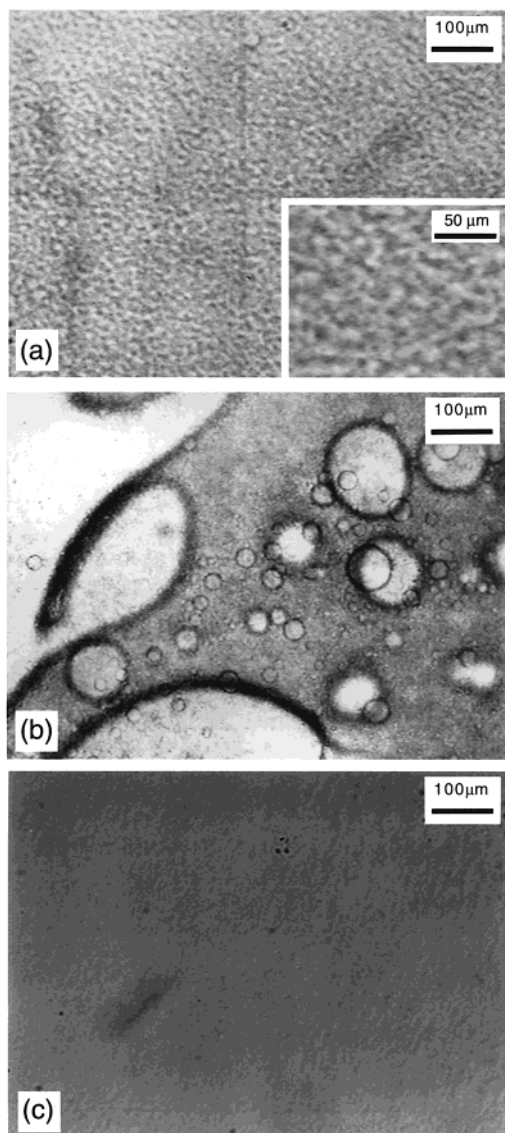


Figure 13. Optical microscope images for the i-2K/s-3K = 50/50 blend. All the images were obtained from the experiments whose thermal programs are given in Figure 9b. Parts a, b, and c correspond to the specimens at “state 1”; “state 2”, and “state 3”, as designated in Figure 9b.

OM with the annealing experiments provide the most clear evidence of the high-temperature (e.g., at 150 °C) immiscibility and the low-temperature (e.g., at 70 °C) miscibility of i-2K and s-3K.

IV. Further Discussion

IV. 1. Estimation of χ -Parameter for Neat Diblock Copolymers. To compare our experimental results with the phase diagram calculated by Matsen and Bates using SCF theory,²⁶ we need to know the temperature dependence of χ parameters for each block copolymer employed in this study. This piece of information was obtained by comparing experimentally measured intensity in the disordered state with the scattered intensity predicted by Leibler's mean-field (MF) theory.⁴⁰ It should be noted that the Leibler's MF theory employed here takes into account the effect of molecular weight polydispersity and asymmetry in a segmental volume as detailed in ref 41. The fitting parameters used to estimate the χ parameter are summarized in Table 2,

Table 2. Characteristic Parameters Used for Estimation of χ -Values in Eqs 1–3 in the Text

code	w_{PS}^a	$N_{PS,n}^b$	$N_{PI,n}^b$	λ^c	$r_{c,n}^d$	χ_s^e
i-2K	0.83	96.2	29.4	1.08	135	0.183
i-3K	0.77	96.2	44.1	1.08	148	0.110
s-3K	0.23	28.9	147.1	1.09	162	0.134

^a w_{PS} is the weight fraction of PS block chain. ^b $N_{k,n}$ is the number-average degree of polymerization of the k th block chain ($k = PS$ or PI). ^c $\lambda = [(M_w/M_n - 1)/(w_{PS}^2 + w_{PI}^2)] + 1$, $w_{PI} = 1 - w_{PS}$. ^d $r_{c,n}$ is the number-averaged effective total degree of polymerization defined by eq A7 of ref 36. ^e χ_s is the χ value at the mean-field spinodal point.

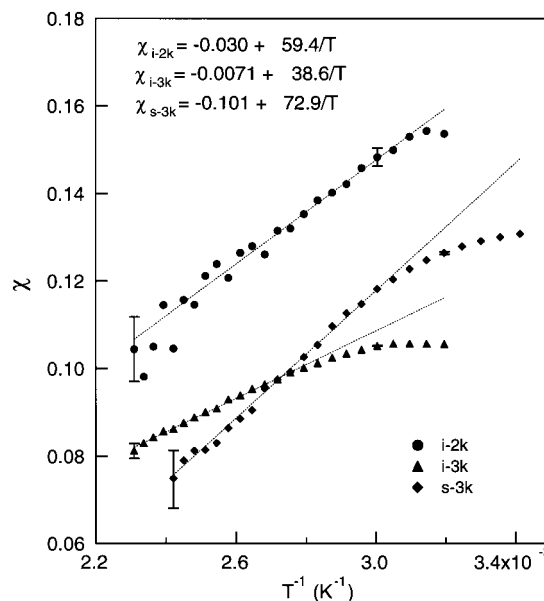


Figure 14. Temperature dependence of χ for each neat diblock copolymer obtained by the RPA analysis of the scattering profiles in the disordered state: (●) i-2K; (▲) i-3K; (◆) s-3K.

and the fitting procedure employed here is exactly same as described in ref 36.

In Figure 14, we show the χ parameters for the three neat copolymers, namely, i-2K, i-3K, and s-3K, which are determined by the fitting procedure, as a function of reciprocal of absolute temperature (T^{-1}). Although the χ parameter of each neat copolymer keeps a linear variation with T^{-1} at small T^{-1} region as anticipated by a relatively good applicability of the MF theory at the high-temperature region far above ODT, the deviation from the linearity was found to occur with further increasing T^{-1} . Two possibilities can be considered for the deviation of χ parameter from the linearity: one is due to the effect of the glass transition of the PS-block,^{34,35} and the other is due to the crossover from the MF type behavior to the non-MF type behavior in the disordered state induced by the thermal noise effect.³⁶ Concerning the PS-rich copolymers, i.e., i-2K and i-3K, the effect of the glass transition cannot be ignored due to the relatively high T_g of PS-block (at around 60 °C³⁵). Therefore, for i-2K and i-3K the suppression of χ at lower temperatures seems to be caused by the effect of T_g . On the other hand for the PI-rich copolymer, s-3K, the effect of T_g is relatively small due to the very small molecular weight of PS-block and the bending in χ with increasing T^{-1} seems to be interpreted as a consequence of the thermal noise effect on the composition fluctuations.^{36,42–45} In any case, both the effect of T_g and thermal noise can be ignored at high enough temperatures. Therefore, we determined the temperature dependencies of χ by using

only a portion of χ vs T^{-1} in which the linearity between χ and T^{-1} is obtained at the high T region.

From Figure 14, the linear part of χ vs T^{-1} is expressed by

$$\chi = -0.030 + 59.4/T \quad (1)$$

for i-2K

$$\chi = -0.0071 + 38.6/T \quad (2)$$

for i-3K, and

$$\chi = -0.101 + 72.9/T \quad (3)$$

for s-3K, respectively. Furthermore, for comparison we cite one expression of χ from ref 46, where a nearly symmetric PS-PI, designated as OSI-3, with $M_n = 1.5 \times 10^4$ and $f_{PS} = 0.45$ was employed.

$$\chi = -0.019 + 32.0/T \quad (4)$$

Although the coefficients A and B in the expression $\chi = A + B/T$ in eqs 1–4, which correspond to the entropic part and the enthalpic part of χ , respectively, are relatively scattered, we can perceive one tendency that the value B becomes large with increasing the asymmetry in the composition of block copolymers (i.e., in the order OSI-3, i-3K, i-2K): It is worthy to note that this tendency is consistent with the previous report.⁴⁷ On the other hand, we cannot find any clear tendencies with respect to the value A .

IV. 2. Comparison of Experimental Results with Calculated Phase Diagram. Matsen and Bates²⁶ explored binary blends of AB diblock copolymers where the total polymerization indices of both copolymers are identical to and designated as N , but the fractions of A-block in the two diblock copolymer species are different, designated as f_1 and f_2 , respectively. Using SCF theory, they compared the thermodynamic stabilities of the “classical” block copolymer phases, i.e., lamellae (L), hexagonally packed cylinders (H), body-centered cubic sphere (C), and disordered phases (D) in the parameter space of χN and ϕ , where ϕ denotes the volume fraction of block copolymer species 2, and mapped phase diagrams.²⁶ The resulting χN vs ϕ diagrams for the pairs of diblock copolymers, with complementary compositions of $f_1 (= 1 - f_2)$ smaller than 0.3, are shown in Figures 3 and 4 of ref 26. Note that in the case of $0.3 < f_1 = 1 - f_2 < 0.7$, the one-component approximation works well: namely, the phase behavior (or morphology) of the binary blend of the block copolymers, whose mean fraction of A-block is equal to $\bar{f} = (1 - \phi)f_1 + \phi f_2$, is nearly identical with that of pure diblock copolymer having the corresponding A-block fraction \bar{f} . However, when $f_1 (= 1 - f_2)$ is reduced to 0.20, the situation drastically changes, as presented in Figure 4 of ref 26. For the 50:50 blend, with increasing χN from the disordered phase, the two constituent copolymers start macroscopically phase-separating at $\chi N \approx 6$ and the two diblock copolymers remain macroscopically phase-separated and do not mix with each other for $6 \leq \chi N \leq 14.6$.²⁶ However, they form a single phase of ordered lamella for $\chi N > 14.6$.

Now, we qualitatively compare our experimental results of i-2K/s-3K = 50/50 with the calculated phase diagram presented in Figure 4 of ref 26, since the condition that f_{PS} of i-2K and s-3K are 0.81 and 0.21, respectively, is similar to that of $f_1 = 1 - f_2 = 0.2$ in the

reference. As described in section III, we determined the macrophase transition temperature of the blend between 125 and 130 °C. This macrophase transition temperature can be expressed in terms of the χN value for the constituent block copolymers for a comparison of the theoretical prediction. At 125 °C, the $\chi r_{c,n}$ values of i-2K and s-3K, evaluated from eqs 1 and 3, are 16.1 and 13.3. $r_{c,n}$ is the number-averaged effective total degree of polymerization defined by eq A7 of ref 36. Thus, assuming that we can take an arithmetic average in $\chi r_{c,n}$, for the i-2K/s-3K = 50/50 blend, we obtain $\chi r_{c,n} = 14.7$, and this result is roughly consistent with the theoretical prediction of $\chi N = 14.6$ for the transition point between the macrophase separation and the microphase separation.

Some differences between the theory and the experiment are also noted. For example, at the region where χN is larger than 14.6, the calculated phase diagram shows lamellar microdomain morphology, whereas the i-2K/s-3K = 50/50 blend at the corresponding region does not suggest a clear morphology with long-range order in the sense that there are no higher-order peaks or shoulders in the SAXS profiles (Figure 4b). Furthermore, the TEM picture (Figure 7f) obtained from the blend specimen, which was held at temperatures below 125 °C but above T_g of PS-rich phase (at around 60 °C³⁵) for more than 12 h, shows the distorted lamellar microdomains without well-developed long-range order.^{48,49} We do not believe that the lack of long-range order arises from insufficient annealing time given to the system to equilibrate, since a prolonged annealing time (longer than 24 h at 70 °C) gave the same result. Almost the same argument is applied for the i-3K/s-3K = 50/50 blend. This discrepancy between the theory and the experiment may arise from the following reason: the theory does not take the thermal fluctuations^{50,51} into account at all, despite the fact that it gives a significant effect in the real systems. It would be worthwhile to experimentally confirm whether or not we can attain the morphological change with decreasing temperature, from the single phase with local order to the single phase of lamellae with long-range order by using a pair of the block copolymers having a slightly larger value of $f_1 = 1 - f_2$ and/or $N = N_1 \cong N_2$. This kind of experimental study deserved a future work.

Another difference between the theory and the experiment is that in the theoretical phase diagram we can find the transition from the macrophase-separated disordered state to the single-phase disordered state with decreasing χN below $\chi N \approx 6$ or increasing temperature above the critical temperature T_c , whereas for our blend we could not observe the corresponding transition with further increasing temperature. Here we would like to note that the spinodal point for the macrophase transition between the two phases in which each phase still has disordered copolymers can be predicted in the context of simple RPA theory and given by^{5,7}

$$2\chi_{\text{eff},s} = \frac{1}{N_1\phi_1} + \frac{1}{N_2\phi_2} \quad (5)$$

where $\chi_{\text{eff},s}$ is the effective segmental interaction parameter (χ_{eff}) of the block copolymer species 1 and 2 at the spinodal point, N_i and ϕ_i ($i = 1$ or 2) denote the polymerization index and the volume fraction of i th block copolymer, respectively, and χ_{eff} is given by

$$\chi_{\text{eff}} = \chi(f_1 - f_2)^2 \quad (6)$$

Since the situation considered in the theory corresponds to $N_1 = N_2 = N$ and $\phi_1 = \phi_2 = 0.5$ we obtain $\chi_{\text{eff},s}N = 2$. Furthermore, since $f_1 = 1 - f_2 = 0.2$, we can derive $\chi_s N \equiv \chi_{\text{eff},s}N/(f_1 - f_2)^2 = 5.56$ at the spinodal point, and this value is identical with that calculated in Figure 4 of ref 26. The corresponding χ_s value at the spinodal point for the mixture having polydispersity in degree of polymerization and asymmetry in segmental volume can be more rigorously evaluated by the following equation

$$2\chi_{\text{eff},s} = \frac{1}{r_{w,1}\phi_1} + \frac{1}{r_{w,2}\phi_2} \quad (7)$$

together with eq 6. In eq 7, $r_{w,i}$ ($i = 1$ or 2) denotes the weight-averaged effective degree of polymerization of block copolymer species i . In the calculation of χ_s based on eq 7, we regarded the block copolymer species 1 and 2 as s-3K and i-2K, respectively, and used the following values: $f_1 = 0.21$, $f_2 = 0.81$, $r_{w,1} = 173$, $r_{w,2} = 143$, $\phi_1 = 0.52$, and $\phi_2 = 0.48$. Consequently, we obtained $\chi_s = 0.0357$ at the spinodal point. Although a large number of studies have been done on the estimation of χ -parameter between PS and PI,⁵² if we adopt the χ vs T relationship for example

$$\chi = 71.4/T - 0.0857 \quad (8)$$

as reported by Rounds,⁵³ where T is absolute temperature, we attain $\chi_s = 0.0357$ at a very high temperature of 315 °C. However, to prevent the cross-linking and/or thermal degradation of the specimen, we have not done any measurements at the temperatures above 150 °C for i-2K/s-3K = 50/50. Thus, the absence of the transition for the i-2K/s-3K = 50/50 blend may be due to the transition point being located at an inaccessibly high temperature in the experimental system.

The points of agreement and disagreement between the theory and the experiment for i-3K/s-3K = 50/50 blend, are nearly identical with those observed for i-2K/s-3K = 50/50 blend. From SAXS profiles (see Figure 5) and TEM micrographs (see Figure 8, parts a and b), we observe that the two copolymers i-3K and s-3K are mixed on the molecular level and do not form any distinct ordered microdomain morphology but remain in the disordered state induced by the thermal fluctuations^{50,51} at the temperature range between 150 and 60 °C, which corresponds to the range of the weight-averaged $\chi_{c,n}$ value for i-3K/s-3K = 50/50 blend between 12.0 and 17.6. Whereas on the theoretical side, although we cannot find the calculated phase diagram for the pair of diblock copolymers with $f_1 = 0.75$ and $f_2 = 0.21$, Figures 3 and 4 of ref 26 allow us to speculate that the SCF theory gives the single L (lamellar) morphology for the condition of $\chi N \geq 12$, $f_1 = 0.75$, $f_2 = 0.21$, and $\phi \approx 0.5$. Therefore, the point of agreement between the experiment and the theory is that we experimentally observed the single phase mixture without macrophase separation at temperatures from 150 °C to room temperature, corresponding to the single phase region of microphase-separated or ordered state in the theoretical phase diagram. The theoretical and experimental results together may further infer that the blend will not undergo the macrophase separation even above 150 °C and in the whole temperature range. While the disagreement point between the theory and the experiment is the morphology: the experimental result did not show

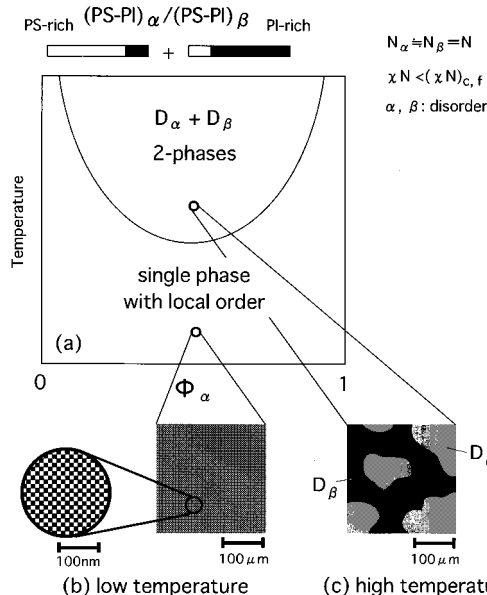


Figure 15. Schematic representation of the phase diagram of the i-2K/s-3K = 50/50 blend in the parameter space of ϕ_α and T (part a), and expected morphologies of the blend specimen at low (part b) and high (part c) temperatures. Note that the phase diagram is effective only for $\phi_\alpha \approx 0.5$.

the distinct morphology with long-range order but the morphology with local order only, contrary to the theoretical prediction of the morphology with long-range order.

The difference in the phase behavior between the two blend systems, the macrophase separation for i-2K/s-3K vs no macrophase separation for i-3K/s-3K, was accounted for by the theory. For a qualitative base, this difference may be best interpreted in terms of the difference of f_{PS} between i-2K and s-3K, the lesser mismatch in the composition of i-3K against s-3K compared with i-2K making the blend i-3K/s-3K more miscible than the blend i-2K/s-3K for the macrophase separation.

V. Concluding Comments

We have investigated the phase behaviors for the binary blends of PS-PI diblock copolymers having the nearly same number-average molecular weights (M_n) but a different volume fraction of PS-block (f_{PS}). One blend specimen with the 50/50 (w/w) blend composition of PS-rich copolymer (i-2K), having $M_n = 1.2 \times 10^4$ and $f_{PS} = 0.81$, and PI-rich copolymer (s-3K), having $M_n = 1.3 \times 10^4$ and $f_{PS} = 0.21$, behaved as if they were the LCST (lower critical solution temperature) type polymer blend as schematically highlighted in Figure 15a. That is, the constituent copolymers, i-2K and s-3K, were mixed on the molecular level at the temperatures below 125 °C, as shown schematically in Figure 15b, and macroscopically phase-separated in the two disordered phases, i.e., the phase rich in α (D_α) and the phase rich in β (D_β) at temperatures above 130 °C, as shown schematically in Figure 15c. The origin of the miscibility of i-2K and s-3K at lower temperatures can be attributed to the local segregation of the repulsive PS and PI segments of both i-2K and s-3K into the PS and PI microdomains (as schematically illustrated in the inset of Figure 15b), driven by the increased χ parameter between the PS and PI segments with decreasing temperature. It should be noted that Figure 15 should be referred only to highlight the “pseudo LCST type

phase diagram" for the particular mixture studied in this work but not necessarily to highlight the other blends in general.

The phase transition between the macroscopically phase-separated state and the single phase composed of microphase-separated state was also predicted by the calculation using the self-consistent field (SCF) theory.²⁶ The calculation of ref 26 and our experiment were in good agreement on the critical χN value at the transition point. However, the discrepancy between the calculation of ref 26 and our experiment was observed in regard to the morphology of microphase-separated state: the calculation predicted the direct transition from the macroscopically phase-separated state to the single phase composed of ordered lamellar microdomain morphology, whereas the 50/50 blend of i-2K and s-3K showed a single phase composed of locally ordered morphology⁴⁸ over the wide temperature range, suggesting that the effect of thermal fluctuations on the ordering was significant for the blend specimen employed in this study.

Acknowledgment. This work was financially supported in part by a Grant-in-Aid for Scientific Research (under Grant No. 12305060(A) and Grant No. 12640392-(C)) from the Ministry of Education, Science, and Culture, Japan. This work is partially supported also by the national project, which has been entrusted to the Japan Chemical Innovation Institute (JCII) by the New Energy and Industrial Technology Development Organization (NEDO) under MITI's Program for the Scientific Technology Development for Industries that Creates New Industries.

References and Notes

- Hashimoto, T. In *Thermoplastic Elastomers, A Comprehensive Review*; Legge, N. R., Holden, G., Schroeder, H. E., Eds.; Hanser: Munich, Germany, 1996; p 429. Hasegawa, H.; Hashimoto, T. In *Comprehensive Polymer Science, Second Supplement*; Aggarwal, S. L., Russo, S. Vol. Eds.; Pergamon: Oxford, England, 1996; p 497.
- Bates, F. S.; Fredrickson, G. H. *Annu. Rev. Phys. Chem.* **1990**, *41*, 525.
- Hadzioannou, G.; Skoulios, A. *Macromolecules* **1982**, *15*, 267.
- Hashimoto, T. *Macromolecules* **1982**, *15*, 1548.
- Hashimoto, T.; Yamasaki, K.; Koizumi, S.; Hasegawa, H. *Macromolecules* **1993**, *26*, 2895.
- Hashimoto, T.; Koizumi, S.; Hasegawa, H. *Macromolecules* **1994**, *27*, 1562.
- Koizumi, S.; Hasegawa, H.; Hashimoto, T. *Macromolecules* **1994**, *27*, 4371.
- Vilesov, A. D.; Floudas, G.; Pakula, T.; Melenevskaya, E. Y.; Birshtein, T. M.; Lyatskaya, Y. V. *Macromol. Chem. Phys.* **1994**, *195*, 2317.
- Floudas, G.; Vlassopoulos, D.; Pitsikalis, M.; Hadjichristidis, N.; Stamm, M. *J. Chem. Phys.* **1996**, *104*, 2083.
- Court, F. These de Doctorat de l'Université Pierre et Marie Curie, 1996.
- Zhao, J.; Majumdar, B.; Schulz, M. F.; Bates, F. S.; Almdal, K.; Mortensen, K.; Hajduk, D. A.; Gruner, S. M. *Macromolecules* **1996**, *29*, 1204.
- Spontak, R. J.; Fung, J. C.; Braunfeld, M. B.; Sedat, J. W.; Agard, D. A.; Kane, L.; Smith, S. D.; Satkowski, M. M.; Ashraf, A.; Hajduk, D. A.; Gruner, S. M. *Macromolecules* **1996**, *29*, 4494.
- Lin, E. K.; Gast, A. P.; Shi, A. C.; Noolandi, J.; Smith, S. D. *Macromolecules* **1996**, *29*, 5920.
- Kane, L.; Satkowski, M. M.; Smith, S. D.; Spontak, R. J. *Macromolecules* **1996**, *29*, 8862.
- Sakurai, S.; Umeda, H.; Yoshida, A.; Nomura, S. *Macromolecules* **1997**, *30*, 7614.
- Sakurai, S.; Irie, H.; Umeda, H.; Nomura, S.; Lee, H. H.; Kim, J. K. *Macromolecules* **1998**, *31*, 336.
- Papadakis, C. M.; Mortensen, K.; Posselt, D. *Eur. Phys. J. B* **1998**, *4*, 325.
- Koneripalli, N.; Levicky, R.; Bates, F. S.; Matsen, M. W.; Satija, S. K.; Ankner, J.; Kaiser, H. *Macromolecules* **1998**, *31*, 3498.
- Bodycomb, J.; Yamaguchi, D.; Hashimoto, T. *Polym. J.* **1996**, *28*, 821.
- Milner, S. T.; Witten, T. A.; Cates, M. E. *Macromolecules* **1989**, *22*, 853.
- Birshtein, T. M.; Liatskaya, Y. V.; Zhulina, E. B. *Polymer* **1990**, *31*, 2185. Zhulina, E. B.; Birshtein, T. M. *Polymer* **1992**, *33*, 1299. Zhulina, E. B.; Lyatskaya, Y. V.; Birshtein, T. M. *Polymer* **1992**, *33*, 332. Lyatskaya, Y. V.; Zhulina, E. B.; Birshtein, T. M. *Polymer* **1992**, *33*, 343. Birshtein, T. M.; Lyatskaya, Y. V.; Zhulina, E. B. *Polymer* **1992**, *33*, 2750.
- Shi, A.-C.; Noolandi, J. *Macromolecules* **1994**, *27*, 2936.
- Spontak, R. J. *Macromolecules* **1994**, *27*, 6363.
- Shi, A.-C.; Noolandi, J. *Macromolecules* **1995**, *28*, 3103.
- Matsen, M. W. *J. Chem. Phys.* **1995**, *103*, 3268.
- Matsen, M. W.; Bates, F. S. *Macromolecules* **1995**, *28*, 7298.
- Hashimoto, T.; Tanaka, H.; Hasegawa, H. *Molecular Conformation and Dynamics of Macromolecules in Condensed Systems*; Nagasawa, M., Ed.; Elsevier: Amsterdam, 1988; p 257.
- Hashimoto, T.; Suehiro, S.; Shibayama, M.; Saijo, K.; Kawai, H. *Polym. J.* **1981**, *13*, 501.
- Suehiro, S.; Saijo, K.; Ohta, Y.; Hashimoto, T. *Anal. Chim. Acta* **1986**, *189*, 41.
- Fujimura, M.; Hashimoto, T.; Kawai, H. *Mem. Fac. Eng., Kyoto Univ.* **1981**, *43* (2), 224.
- Hendricks, R. W. *J. Appl. Crystallogr.* **1972**, *5*, 315.
- Kato, K. *J. Polym. Sci., Polym. Lett. Ed.* **1996**, *4*, 35.
- Hashimoto, T.; Kumaki, J.; Kawai, H. *Macromolecules* **1983**, *16*, 641.
- Yamaguchi, D.; Hashimoto, T.; Han, C. D.; Baek, D. M.; Kim, J. K.; Shi, A.-C. *Macromolecules* **1997**, *30*, 5832.
- We have checked that both i-2K and i-3K have their T_g 's in the relatively broad temperature range 40–60 °C, by differential scanning calorimetry (DSC) measurements.
- Sakamoto, N.; Hashimoto, T. *Macromolecules* **1995**, *28*, 6825.
- The use of ice water to quench the specimens is sufficient, because the change of the structures of our interest induced by lowering temperature is very slow.
- One possible origin for the chatter in Figure 7 may be due to the big difference in rigidities of i-2K-rich and s-3K-rich domains.
- Although the data are not shown here, we have checked that i-3K and s-3K were still miscible on the molecular level up to 190 °C on the heating process.
- Leibler, L. *Macromolecules* **1980**, *13*, 1602.
- Sakurai, S.; Mori, K.; Okawara, A.; Kimishima, K.; Hashimoto, T. *Macromolecules* **1992**, *25*, 2679.
- Hashimoto, T.; Ijichi, Y.; Fetter, L. J. *J. Chem. Phys.* **1988**, *89*, 2463. Ijichi, Y.; Hashimoto, T.; Fetter, L. J. *Macromolecules* **1989**, *22*, 2817.
- Holzer, B.; Lehman, A.; Stühn, B.; Kowalski, M. *Polymer* **1991**, *32*, 1935.
- Floudas, G.; Pakula, T.; Fischer, E. W.; Hadjichristidis, N.; Pispas, S. *Acta Polym.* **1994**, *45*, 176.
- Lin, C. C.; Jonnalagadda, S. V.; Kesani, P. K.; Dai, H. J.; Balsara, N. P. *Macromolecules* **1994**, *27*, 7769.
- Koga, T.; Koga, T.; Hashimoto, T. *J. Chem. Phys.* **1999**, *110*, 11076.
- Mori, K.; Okawara, A.; Hashimoto, T. *J. Chem. Phys.* **1996**, *104*, 7765.
- Sakamoto, N.; Hashimoto, T. *Macromolecules* **1998**, *31*, 3815.
- Sakamoto, N.; Hashimoto, T. *Macromolecules* **1998**, *31*, 3292.
- Brazovskii, A. *Sov. Phys. JETP* **1975**, *41*, 85.
- Fredrickson, G. H.; Helfand, E. *J. Chem. Phys.* **1987**, *87*, 697.
- See for example, refs 42 and 45, and as follows: Mori, K.; Tanaka, H.; Hasegawa, H.; Hashimoto, T. *Polymer* **1989**, *30*, 1389. Owens, J. N.; Gancarz, I. S.; Koberstein, J. T.; Russell, T. P. *Macromolecules* **1989**, *22*, 3380. Hashimoto, T.; Mori, K. *Macromolecules* **1990**, *23*, 5347. Stuhn, B. *J. Polym. Sci., Polym. Phys. Ed.* **1992**, *30*, 1013. Balsara, N. P.; Perahia, D.; Safinya, C. R.; Tirrell, M.; Lodge, T. P. *Macromolecules* **1992**, *25*, 3896. Jian, T.; Anastasiadis, S. H.; Fytas, G.; Adachi, K.; Kotaka, T. *Macromolecules* **1993**, *26*, 4706. Balsara, N. P.; Lin, C. C.; Dai, H. J.; Krishnamoorti, R. *Macromolecules* **1994**, *27*, 1216. However the general conclusion that the value of $\chi = 0.0357$ corresponds to a very high temperature hardly depends on the choice of various reported results on χ vs T .
- Rounds, N. A. Ph.D. Dissertation, University of Akron, 1970.